

Research Article

Chemical Shrinkage During Hydration Reactions of Calcium Aluminate Cement

Ukrainczyk N*

Faculty of Chemical Engineering and Technology,
University of Zagreb, Croatia*Corresponding author: Ukrainczyk N, Faculty of
Chemical Engineering and Technology, University of
Zagreb, Marulićev trg 20, 10 000 Zagreb, CroatiaReceived: October 07, 2014; Accepted: October 24,
2014; Published: October 27, 2014**Abstract**

Calcium Aluminate Cement (CAC) is special cement used in versatile high performance applications. Hardening of CAC is primarily due to the hydration of mono-calciumaluminate, in idealized pure form CaAl_2O_4 , but other minerals also participate in the hydration process especially at higher temperatures and in long term. During the hydration reactions of cement, absolute volume of hydration products formed is smaller than that of its reactants, cement and water, resulting in chemical shrinkage. Chemical shrinkage is the main driving mechanism leading to desiccation and early age cracking of cement based materials. Its evolution is an overall result of complex kinetics of many simultaneous hydration reactions. Even same minerals can have different reaction schemes due to the transformation process of metastable hydration products to the stable ones, which are promoted by temperature.

In this paper the hydration of synthetic CaAl_2O_4 and commercial iron-rich CAC were investigated at 15 and 55 °C by measurements of chemical shrinkage evolution and quantitative powder X-ray diffraction analysis. Design of an experimental configuration for measuring the chemical shrinkage during CAC hydration is discussed. A model is proposed to predict the evolution of chemical shrinkage during hydration. The model is based on the main chemical reaction schemes of the CAC hydration and showed good agreement with the observed experimental results.

Keywords: Calcium aluminate cement; Hydration; Chemical shrinkage; X-ray diffraction; Mathematical modeling

Abbreviations

CAC: Calcium Aluminate Cement; PC: Ordinary Portland Cement; C: CaO (cement chemistry notation); A: Al_2O_3 ; F: Fe_2O_3 ; S: SiO_2 ; H: H_2O ; CA: CaAl_2O_4 ; C_{12}A_7 : $\text{Ca}_{12}\text{Al}_{14}\text{O}_{33}$; C_4AF : $\text{Ca}_4\text{Al}_2\text{Fe}_2\text{O}_{16}$; Ff: Ferrite Phase (C_4AF); CT: CaTiO_3 ; $v_{\text{H}_2\text{O}}$: Specific Volume of Water; v_{m} : Specific Volume Of Cement Mineral; v_{hydrates} : Volume of the formed hydration products per 1 g of reacted mineral m ; m : cement mineral: CA, C_{12}A_7 or C_4AF ; h : hydration product: CAH_{10} , C_2AH_8 , C_3AH_6 , AH_3 , FH_3 , CH or $\text{C}_4\text{AFH}_{16}$; stoichiometric coefficient; M : Molar Mass; ρ : density; CS_m : Chemical Shrinkage of fully reacted pure mineral m ; α_m : fraction of reacted mineral m ; w_m mass fraction of the mineral m in cement; W : Weight; V : Volume; V_{paste} : the Volume change of the cement paste; t : time.

Introduction

Calcium Aluminate Cement (CAC) is special cement used in versatile high performance applications [1-8] such as those requiring: resistance to chemical attack, high early strength, refractory, resistance to abrasion, and/or low ambient temperature placement. Setting and hardening of CAC is primarily due to the hydration of CA (cement chemistry notation: C=CaO, A= Al_2O_3 , F= Fe_2O_3 , S= SiO_2 , H= H_2O), but other compounds also participate in the hardening process especially in long term strength development [1,2] and at higher temperatures of hydration. The hydration of CAC is highly temperature dependent [1-3,9], yielding CAH_{10} as main products at temperatures less than 20 °C, C_2AH_8 and AH_3 at about 30 °C, and

C_3AH_6 and AH_3 at temperatures greater than 55 °C. Platy (hexagonal) CAH_{10} and C_2AH_8 [10] are metastable at ambient temperature and convert to the more stable C_3AH_6 and AH_3 with consequent material porosity and permeability increase and loss of strength [1]. The conversion is accelerated by temperature and moisture availability.

Chemical shrinkage occurs during cement hydration reactions because the absolute volume of hydration products formed is smaller than that of its reactants, cement and water (i.e. $v_{\text{hydrates}} < v_{\text{cement}} + v_{\text{H}_2\text{O}}$). Chemical shrinkage is generally considered as the main driving mechanism (at microscopic scale) leading to early age cracking and, thus, to the loss of durability of cement based materials at macroscopic scale (e.g. concrete structures) [11-13]. The external (macroscopic) dimensional shrinkage of cement based materials is very similar to the chemical shrinkage until the establishment of a semi-rigid skeleton around setting time [11]. After setting time chemical shrinkage results in vapor filled internal porosity that develops capillary related internal stresses. To quantify chemical shrinkage, cement paste specimen must be kept water saturated so the imbibed external water needed to replace the volume decrease can be measured. Techniques for measuring chemical shrinkage and the discussion on systematic errors and critical design of an experimental configuration are presented in next section (*Chemical shrinkage tests*).

There is a lack of knowledge related to the volume change behaviour of CAC. Recently, Ideker et al. [12,13] studied the early-age volume change behaviour during hydration of low-iron grade CAC.

To the best of our knowledge there are no experimental data showing the evolution of the chemical shrinkage during pure CA and iron-rich CAC hydration. Chemical shrinkage evolution is an overall result of complex kinetics of many reactions of several cement minerals. Even same minerals can have different reaction schemes due to the transformation process of metastable hydration products to the stable ones, whose rate is increasing with temperature. Mounanga et. al. [14] successfully described chemical shrinkage evolution during hydration of Portland cement. The information about hydration kinetics of individual minerals during CAC hydration is not yet fully available [15]. In literature there is still not yet an adequate cement paste model for CAC hydration analog to PC hydration [14]. However, in first approximation the early age of CAC hydration, especially at lower temperatures ($T < 20^{\circ}\text{C}$) could be described by hydration reactions of the principal minerals [15,16]. This paper comes within the scope of a larger study conducted to build a model for CAC hydration that requires complementary experimental results on evolution of various properties. For this non-destructive continuous experimental tests are desired, such as calorimetry [7,15,17], chemical shrinkage, thermal properties [9], ultrasonic wave propagation [18,19], which need to be combined with destructive tests to determine the chemically bounded water [10,20], fractions of reacted cement minerals [15], hydration products formed [8], density of the cement paste solids (volume fraction of the solids) [18], porosity, and strength [8,17,18].

In this paper the hydration of synthetic CaAl_2O_4 and commercial iron-rich calcium aluminate cement were investigated by Quantitative Powder X-Ray Diffraction (QXRD) analysis and measurements of chemical shrinkage evolution. A model is proposed to predict the evolution of chemical shrinkage during hydration based on the main chemical reaction schemes of the CAC hydration. The model predictions of the chemical shrinkage hydration are compared to the experimental results.

Chemical shrinkage tests

There are three basic techniques for measuring chemical shrinkage: dilatometry, pycnometry and gravimetry [11,21,22]. In dilatometry test procedure a drop of water level in a capillary tube above a specimen is monitored manually or automatically [23]. Pycnometry consists of a pycnometer filled with paste and water on top. At different ages water is added to refill the pycnometer, and the weight increase relates to the total volume change. In gravimetric test procedure the volume change due to water imbibition in the hydrating specimen is obtained by measuring submerged weight according to Archimedes law. This paper employed the gravimetric method that is relatively simple to automate and is described in detail in section *Chemical shrinkage measurement*.

Recent review of chemical shrinkage methods in cement based materials at early ages is given in [11]. The test methods for measuring chemical shrinkage have experimental difficulties that must be adequately accounted for in order to avoid systematic errors in results. First, the specimen must be thin enough (especially for specimens with low water to cement mass ratio, H/CAC) to easily imbibe the clear water above the cement paste and thus avoid the creation of vapor filled internal porosity created by chemical shrinkage [11,23]. In other words, the rate of water supply (or transfer) from the top to the bottom of the specimen must be higher than the rate of

chemical shrinkage. For Portland cement paste with a low water to cement ratios, this scale effect is not significant for sample thickness inferior to 10 mm during the first 24 h of hydration [14]. Second, the specimen must be de-aired, because the entrapped air bubbles going from water to paraffin change the submerged weight during the measurement. Third, the amount of the clear water above the specimen, and its chemical composition influence the results, especially in initial stage. Larger amount of clear water above the cement paste accelerate the initial reaction because of the dilution of the cement paste pore solution [11]. To obtain measurements on water to cement ratios closer to practical values with lower dilution one should employ paraffin oil as buoyancy fluid. Moreover, as the chemical shrinkage begins instantly upon water contacting cement (during initial mixing), the measurement results depend on the delay of the starting time. The data have to be carefully referenced to the time of starting the measurements which is about ten minutes after mixing the cement with water due to sample preparation. And lastly, the temperature gradients of the sample should be kept low. This is important if the measurements of chemical shrinkage of cements (especially calcium aluminates) are performed at higher temperatures when the reactions rates, and thus the heating rates are high. During the hydration of CAC a large quantity (70-90 % [6-9,15]) of heat is liberated within one day that may cause a considerable increase of temperature in CAC based material. All the aforementioned effects must be considered when designing an experimental set-up and interpreting the results of the chemical shrinkage measurement.

Materials and Methods

Commercial CAC ISTRA 40 was taken from a regular production of *Istra Cement*, Croatia (CALUCEM Group). The cement has the oxide mass fraction composition listed in Table 1. Physical properties of used cement are given in Table 2. The main compounds are CA (45%) and ferrite phase (C_4AF , 21%), with mayenite (C_{12}A_7 , 5%), gehlenite (C_2AS) and $\beta\text{-C}_2\text{S}$ as minor compounds. For the syntheses of CA, ferrite phase and C_{12}A_7 , precipitated calcite (CaCO_3 analytical grade purity, Kemika), gibbsite ($\text{Al}(\text{OH})_3$, Sigma-Aldrich) and Fe_2O_3 have been wet homogenized in planetary mill (FRITTSCH, Pulverisette 5, α -Alumina pot and grinding balls) in the required stoichiometric mole proportion, dried at 105°C and then fired at 1350°C for 3 h in an air atmosphere electric furnace. Synthetic minerals were milled in a ring agate mortar and sieved below $40\ \mu\text{m}$. XRD analysis of the synthesised CA (Figure 1) shows its high crystallinity and purity, with only small traces of detected C_{12}A_7 and corundum. Specific surface of the prepared CA used for chemical shrinkage measurements was $4960\ \text{cm}^2/\text{g}$ (Blaine). Decarbonated and deionised water is used and exposure of the samples to the (CO_2) atmosphere is kept to a minimum.

Table 1: Chemical composition of investigated CAC.

CaO	Al_2O_3	Fe_2O_3	FeO	SiO_2	TiO_2	MgO	SO_3	Na_2O	K_2O	Sum
37.1	38.5	14.4	2.9	4.4	1.1	0.9	0.2	0.14	0.17	99.81

Table 2: Physical properties of investigated CAC.

>90 μm , %	<40 μm , %	Blaine, cm^2/g	Specific gravity, g/cm^3	Setting time, min		Standard consistency, %
				Initial	final	
3.76	80.50	3508	3.20	298	329	24.0

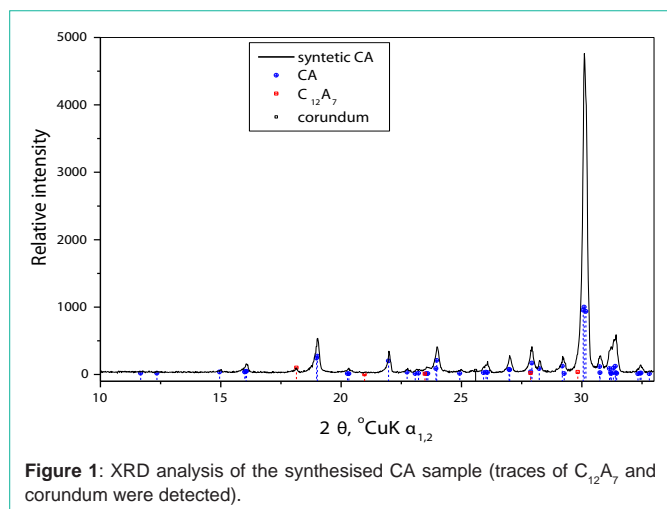


Figure 1: XRD analysis of the synthesised CA₁ sample (traces of C₁₂A₇ and corundum were detected).

Chemical shrinkage measurement

In this study, chemical shrinkage measurements are carried out using a gravimetric method [11,21,23]. The change in buoyancy was continuously monitored for samples suspended in paraffin oil. The illustration of the experimental setup is given in (Figure 2). The samples are prepared in a thin glass sample holder ($2r = 29$ mm and $h = 50$ mm). Firstly, on 8 g of cement the deionized water was added with a medicine dropper to obtain water to cement mass ratio of $H/CAC = 0.5$ and $H/CA = 0.95$ for Istra 40 and synthetic CA, respectively. This paste was mixed by applying vibrations. Secondly, more deionized water was added with a medicine dropper to form a layer of clear water above the cement paste. The overall H/CAC ratio was $H/CAC = 1.0$ and $H/CA = 1.5$ for the Istra 40 and the synthetic CA, respectively. As the measurement necessities the presence of the clear water above the cement paste the overall water to cement ratio was chosen accordingly to compensate the volume changes (water uptake) that are expected during measurement time. The prepared specimens (cement pastes without the clear water above it) are 5 mm thick. Thirdly, specimens were de-aired by placing the filled sample holder in a desiccator. Air was evacuated from the desiccator by using a vacuum pump. During the de-aeration the desiccator was vibrated. Lastly, the paraffin oil is added, initially with a medicine dropper to form a layer above the water, followed by pouring larger quantities of paraffin to almost completely fill the sample holder.

The sample holder is hung on a balance (sensitivity 0.1 mg) by a thread and immersed in a laboratory glass (400 mL) filled with paraffin oil (Figure 2) at the required curing temperature (thermostated 15 L water bath with ± 0.05 °C). Balance is connected to the Personal Computer (PC) via RS232 protocol employing acquisition software. The measurement started 10 min after initial water–cement contact with a sampling rate of 15 s. Appropriate corrections were applied to account for a temperature stabilization of the sample during first minutes of the measurement. This was done by subtracting the baseline obtained by measuring the response of the hydrated sample (stabilized at room temperature) when immersed in a curing temperature of paraffin oil.

The density of used paraffin oil, ρ_{par} was measured (to be 0.850 g/cm³ at 15 °C) by applying Archimedes method and utilizing glass sinker (part of standard equipment for density measurements by

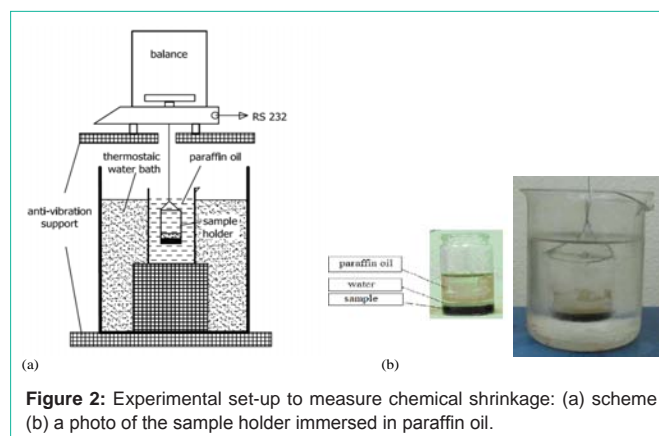


Figure 2: Experimental set-up to measure chemical shrinkage: (a) scheme (b) a photo of the sample holder immersed in paraffin oil.

KERN ALS 220-4 balance):

$$\rho_{\text{par}} = (W_{\text{air}} - W_{\text{par}}) / V_s + \rho_{\text{air}} \quad (2.1)$$

where: ρ_{air} is air density [0.0012 g/cm³], ρ_{par} – density of the paraffin oil [g/cm³], W_{air} – weight of the sinker in air [g], W_{par} – weight of the sinker submerged in the paraffin oil [g], V_s – volume of glass sinker [10.4920 cm³].

Likewise, using the Archimedes law the chemical shrinkage [CS, cm³/g] evolution during cement paste hydration is calculated:

$$CS(t) = \Delta V_{\text{paste}}(t) / W_{\text{cem}} = (W(t) - W(24)) / (\rho_{\text{par}} W_{\text{cem}}) \quad (2.2)$$

where: ΔV_{paste} is the volume change of the cement paste [cm³], t is time, W_{cem} is weight of cement in paste [g], $W(t)$ is weight of the submerged paste at time t [g], $W(24)$ is an initial weight of the submerged paste 24 min after cement-water mixing [g], and ρ_{par} is density of the paraffin oil [g/cm³].

At the end of chemical shrinkage measurements the specimens were removed from the sample holder and crushed to a fine powder. The hydration was blocked and free water removed by addition of acetone (2-propanon). This was done by grinding and mudding the sample in three doses with acetone in agate mortar and CO₂ free atmosphere.

Powder X-ray diffraction

The composition of CAC and hydrates formed was investigated by powder X-Ray Diffraction (XRD). Shimadzu diffractometer XRD-6000 with Cu K_{α1,2} radiation was used (the scan step was 0.02° with collection time of 1 for qualitative and 4 s for quantitative analysis). For Quantitative X-Ray Analysis (QXRD), the prepared hydrated samples were additionally fired at 500 °C (for 10 min) to decompose the hydrates to amorphous oxides and water vapor. Expected amorphous oxides after heating are C₂A(am.) from C₂AH₈, CA(am.) from CAH₁₀, A(am.) from AH₃ and C₃A(am.) from C₃AH₆. By this method, proposed in [15], the interferences of the hydration products are excluded from the diffractograms. This enables a direct determination of the degree of hydration of individual minerals upon comparing the quantities in hydrated and initial (non-hydrated) cement samples. The temperature for decomposition was chosen by inference to thermogravimetry and XRD analysis of hydrated samples [10,15].

CAC quantitative X-ray diffraction using the adiabatic principle

with auto flushing as proposed by Chung [24] is proven to be a suitable method [25]. Here, the matrix-flushing method [24] was applied as it enables to directly quantify relative portions in sample including both the crystalline and amorphous components by analyzing for only those components of interest. Here only CA, $C_{12}A_7$ and C_4AF , while quantification of other minerals (e.g. pleochroite, C_2AS , C_2S , FeO, CT) and amorphous phases was and can be omitted. The criterion for this method is that the reference material must have the same level of crystallinity (the same level of perfection or imperfection in crystal structure) as the component in the sample. The Full-Width at Half-Maximum (FWHM) of reflections in an X-ray diffraction pattern was compared as an indication of the crystallinity of the components. FWHM for CA was measured from the peak comprising three close reflections at 30.06° , 30.1° and 30.17° and corrected by subtracting it with the width of this reflections (0.11°). The obtained FWHM were 0.17° , 0.16° , 0.12° and 0.16° for rutile (reflection at 27.4°), $C_{12}A_7$ (33.3° and 18.1°), CA and C_4AF (12.2°), respectively. This indicates no significant differences in their crystallinity. It is important to note that the possible effect of the observed difference is lowered by using peak areas instead of peak heights to define/quantify diffraction peak intensity. In the matrix-flushing method the relationship between the peak intensity (peak area) of the characteristic X-ray reflection I_i is directly proportional to the weight fraction of the component by the factor k_i which contains the mass absorption coefficient of the total sample. Experimentally determined k_i values hold only for the detecting system and for no other. Reasonable standard materials for such a study are rutile (TiO_2) [15] or corundum (Al_2O_3) [25]. The rutile used in this study had a narrow particle size distribution around approximately $0.4 \mu m$, which would reduce microabsorption effect. XRD analysis of chosen standard rutile showed no traces of anatase. In this work, CA, $C_{12}A_7$, C_4AF in CAC and fired hydrated samples are quantified based on the matrix-flushing method by Chung. The k_i values were determined by mixing of pure phase and standard mineral rutile (TiO_2) in a 50:50 weigh ratio. Pure synthetic minerals were milled in a ring agate mortar and sieved below $40 \mu m$ to maximize the number of particles analyzed, to improve powder homogeneity and packing characteristics, and to minimize micro absorption-related problems. Each sample prepared for QXRD (0.7 g) was mixed with a fixed amount of rutile (0.14 g), followed by grinding and homogenization in an agate mortar under acetone. Appropriate corrections for peak overlap were meticulously applied by inference to the (measured) intensities of the pattern due to pure phases.

Modeling methodology

If knowing the densities of components (Table 3) and hydration reaction stoichiometry (eqs 1-7 presented in Table 4) the chemical shrinkage of pure minerals (in cm^3/g of mineral) for complete hydration can be calculated as:

$$CS_m = v_H + v_m - v_{hydrates} \quad (8)$$

Where the v_m and v_H is the specific volume of the cement mineral and water, respectively, and $v_{hydrates}$ is the volume of the formed hydration products per 1 g of reacted mineral calculated as:

$$v_{hydrates} = \sum_h \left(\frac{M_h v_h}{M_m v_m \rho_h} \right)_{hydrates} \quad (9)$$

where the sum is for all hydration products (h), v and M

Table 3: Densities and molar masses of the components [5,26,27].

Component	$\rho / g \text{ cm}^{-3}$	$M / g \text{ mol}^{-1}$
CA	2.98	158.1
$C_{12}A_7$	2.85	1387
C_4AF	3.73	485.9
CAH_{10}	1.72	338.1
C_2AH_8	1.96	358.2
C_4AFH_{16}	2.2	774.1
C_3AH_6	2.52	378.3
AH_3	2.44	156.0
FH_3	2.20	213.7
CH	2.24	76.1

Table 4: Theoretical values of chemical shrinkage for complete hydration of mineral upon individual reaction stoichiometry [1,27].

Mineral	Reaction eq.	Eq. no.	Temperature, $^\circ C$	CS, cm^3/g of mineral
CA	$CA + 10 H \rightarrow CAH_{10}$	(1)	15	0.2317
	$2 CA + 11 H \rightarrow C_2AH_8 + AH_3$	(2)	15	0.1821
	$3 CA + 12 H \rightarrow C_3AH_6 + 2 AH_3$	(3)	55	0.2113
$C_{12}A_7$	$C_{12}A_7 + 60H \rightarrow 5C_2AH_8 + 2CAH_{10}$	(4)	15	0.1879
	$C_{12}A_7 + 33H \rightarrow 4C_3AH_6 + 3AH_3$	(5)	55	0.2140
C_4AF	$C_4AF + 10H \rightarrow C_3AH_6 + CH + FH_3$	(6)	55	0.0658
	$C_4AF + 16H \rightarrow C_4AFH_{16}$	(7)	15	0.1343

are stoichiometric coefficient and molar masses of the reaction components, respectively, and ρ_h is the density of hydration product [5,26,27] (Table 3). The volume of the water required for the stoichiometric hydration of the mineral m is:

$$v_H = \frac{M_H v_H}{M_m v_m \rho_H} \quad (10)$$

Table 4 summarizes theoretical values of total chemical shrinkage for complete hydration of mineral upon individual reaction stoichiometry at $T = 15$ and $55^\circ C$. Furthermore, the evolution of chemical shrinkage could be calculated by multiplying the total chemical shrinkage by the degree of reacted mineral.

To model the chemical shrinkage evolution of CAC paste we need to know the hydration reaction stoichiometry (thermodynamics) and reaction kinetics of all cement minerals. This information is not yet fully available due to the complexity of reactions involved during hydration of commercial CAC. However, in first approximation principal hydration reactions can be considered. From these data, the chemical shrinkage (CS in cm^3/g of CAC) versus overall hydration degree (α) of the principal minerals, m can be expressed as:

$$CS(\alpha) = \sum_m CS_m \alpha_m w_m \quad (11)$$

Where: CS_m is the chemical shrinkage of fully reacted pure mineral calculated by eq. 8, α_m is the fraction of reacted mineral (m), and w_m is the mass fraction of the mineral in cement. To predict the chemical shrinkage of CAC by eq. (11), in this paper the hydration of CA, C_4AF and $C_{12}A_7$ is considered upon reaction schemes as shown

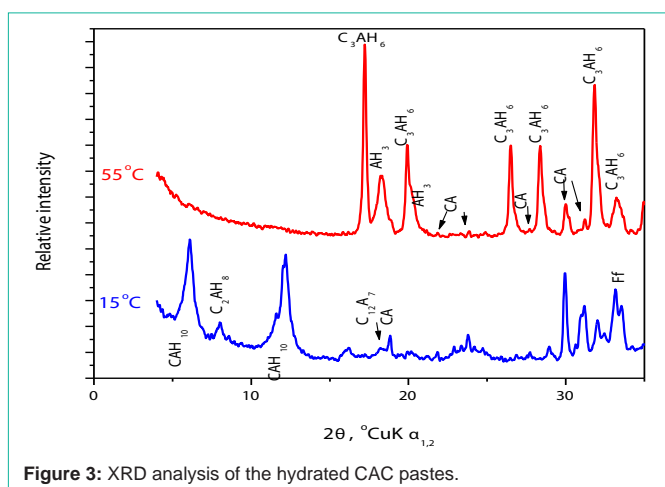


Figure 3: XRD analysis of the hydrated CAC pastes.

in Table 4. At 15 °C ($t < 35$ h) only metastable hydration products are formed, while at 55 °C and sufficient time the conversion is practically completed leaving only stable hydration products. To test the proposed model against the measured chemical shrinkage the amount of reacted CA, C_4AF and $C_{12}A_7$ was quantified by QXRD analysis.

In the case of the iron rich CAC, the most hydraulic phases are CA and $C_{12}A_7$, while C_2AS , C_2S and ferrite phase (nominally C_4AF) are considered to have no significant reactivity at early ages (first 48 hours) below 20 °C [1,5,15]. However, although C_4AF reactivity has usually been disregarded in studies of CAC hydration, because of its high quantities (up to 30 %) one should be careful in considering its contribution.

Results and Discussion

XRD analysis on samples obtained from hydrated specimens cured at different conditions (Figure 3) confirmed the hydrate compositions expected from the literature [1,5,8,15]. The main hydration products observed on specimens hydrated at 15 °C was CAH_{10} with traces of C_2AH_8 and AH_3 . Transformed samples hydrated at 55 °C gave C_3AH_6 and AH_3 as hydrated products. Main diffraction peaks of metastable hydration products and AH_3 are fairly broadened, indicating poor crystallinity, while that of the C_3AH_6 product showed good crystallinity. The QXRD analysis of investigated CAC gave the mass proportions of CA, $C_{12}A_7$ and C_4AF to be 45 %, 5 % and 21 %, respectively. From the QXRD analysis the degree of hydration of CA, $C_{12}A_7$ and C_4AF was obtained and presented in Table 6. It can be observed that the fraction of reacted cement minerals (CA, $C_{12}A_7$ and C_4AF) significantly increased with temperature.

Results of the chemical shrinkage evolution during the hydration of the cement samples (Figure 4) indicate the kinetics of the cement hydration. When cement and water first come in contact the initial hydration is attributed mainly to the cement wetting and dissolution processes. During the induction period a small rate of hydration reaction is observed. Induction period is followed by the onset of the accelerated stage of reaction due to massive precipitation of hydrates. The hydration rate is than again decreasing due to consumption of the reactants and mass transfer limitations [15]. The reason for slower nucleation activity of the CA15 than CAC15 (Figure 4) could be explained by the lack of germination sites for the nuclei to start

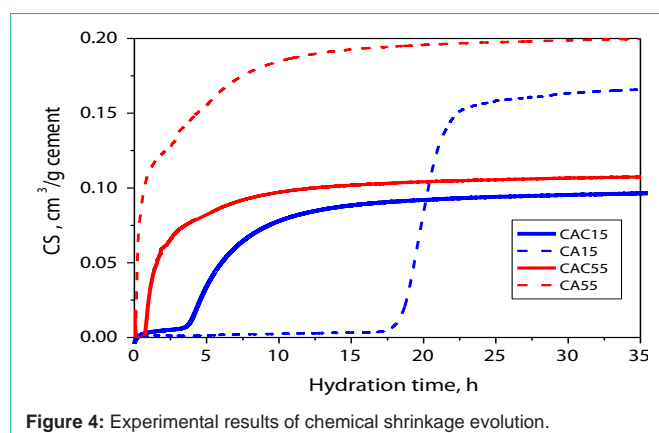


Figure 4: Experimental results of chemical shrinkage evolution.

the precipitation of the metastable hydration products. On the other hand, at 55 °C, the CA55 has higher nucleation activity than CAC55, which can be attributed to the higher specific surface of the synthetic CA. Both the nucleation period and the reaction rate after the onset of the massive precipitation are higher at higher temperature.

Less amount of chemical shrinkage is evolved during the initial (dissolution) stage for CAC than for Portland cement (compared with the experimental results from [11]). This was also observed by calorimetric measurements [7,8,15]. The maximal CAC hydration rate at 15°C (inflection point of the CAC15 curve in Figure 4 at $t_{max} = 4.3$ h), dCS/dt_{max} is $25 \cdot 10^{-3} \text{ cm}^3/(\text{g h})$ which is about ten times greater in comparison to chemical shrinkage results on PC ($dCS/dt_{max,PC} \sim 2.5 \cdot 10^{-3} \text{ cm}^3/(\text{g h})$ [11]). After 35 h of hydration at 15°C chemical shrinkage of CAC ($0.096 \text{ cm}^3/\text{g}$) is more than 2.5 times higher than for PC (about $0.035 \text{ cm}^3/\text{g}$ [11]). If temperature gradients are ensured to be low (below $\sim 1^\circ\text{C}$) the higher hydration rate and achieved hydration degree could enable more accurate measurements of CAC chemical shrinkage in comparison to PC (Table 5). As expected, the obtained values of chemical shrinkage for synthetic CA15 are even higher (Figure 4 and Table 6), about 2.2 times that for CAC15, with a maximal rate dCS/dt_{max} of $0.055 \text{ cm}^3/(\text{g h})$. The lower values of chemical shrinkage for commercial CAC hydration than synthetic CA can be explained mainly by a high amount of slow reacting minerals in the CAC sample. Moreover, CAC has a lower specific surface than CA sample.

Results of the QXRD analysis and the comparison of predicted and measured chemical shrinkage is presented in Table 6. One can see that the model eq. (11) based on the reaction equations (1-7) (Table 4) is in good agreement with the obtained experimental results. The reactivity of other phases but CA, $C_{12}A_7$ and C_4AF has been disregarded in the simplified stoichiometric model to describe chemical shrinkage of CAC. At 15°C it was assumed that C_2AH_8 originates only from hydration of $C_{12}A_7$ (eq. 4), as the conversion of CAH_{10} to C_2AH_8 is very slow at $T \leq 15^\circ\text{C}$ [1-3]. Calculated amount of formed C_2AH_8 in cement paste by reaction eq. 4, considering water to cement mass ratio of 0.5,

Table 5: Experimental plan for investigating the hydration of the cement samples.

Sample label	Cement sample description	T , °C	H/c
CA15	$CaAl_2O_4$	15	1.5
CA55	$CaAl_2O_4$	55	1.5
CAC15	CAC ISTR A 40	15	1.0
CAC55	CAC ISTR A 40	55	1.0

Table 6: Results of the QXRD analysis and the comparison of predicted and measured chemical shrinkage (at hydration time $t_h = 35$ h).

Sample	$\alpha_{C_{12}A_7}$	α_{FF}	QXRD α_{CA}	CS, cm ³ /g of sample		Deviation, %
				Model	Measured	
CA15	-	-	0.72	0.167	0.166	0.5
CA55	-	-	0.97	0.199	0.200	- 0.4
CAC15	0.6	0.08	0.80	0.091	0.096	- 4.9
CAC55	1.0	0.5	0.95	0.108	0.107	0.9

5% of $C_{12}A_7$ in CAC of which 60% has reacted, is 2.6%, in agreement with its relatively very low diffraction peak. However, at longer times and at higher temperatures conversion is significant, and to calculate the chemical shrinkage the ratio of reactions (eqs. 1-3) should be determined, e.g. from ratio of formed hydration products, which is quite challenging. More data are needed to validate the used model for predicting the chemical shrinkage evolution during continuous hydration, especially at higher temperatures. The presented modeling methodology can be extended to develop more complex models to describe all three reactions of CA hydration scheme simultaneously, and even to include other hydraulically active minerals (e.g. $C_{12}A_7$, C_4AF and C_2S). QXRD analysis of cement is difficult as the multiple phases result in substantial peak overlap. There is also difficulty in securing suitable pure phase reference standards. For better accuracy, these concerns may be addressed using the quantitative Rietveld analysis of all CAC phases. More accurate quantitative data on hydration of different CACs should be used to additionally test the proposed model for predicting the evolution of chemical shrinkage during CAC hydration.

Conclusion

Chemical shrinkage test methods have experimental difficulties (outlined in section Chemical shrinkage test) that must be adequately accounted for in order to avoid systematic errors in experimental results. From the chemical shrinkage results obtained the following can be stressed out. After 35 h of hydration chemical shrinkage of CAC is more than 2.5 times higher than for Portland cement but about 2.2 times lower than for synthetic CA. Lower chemical shrinkage evolved during the measurements of commercial CAC than synthetic CA can be attributed mainly to a high amount of slow reacting minerals in the CAC sample, and also to difference in the specific surface of the cement samples. The reason for the faster nucleation activity of the CAC than CA at 15 °C could be explained by more germination sites and the seeded heterogenous nuclei effect. On the other hand, at 55 °C, the synthetic CA has higher nucleation activity than the commercial CAC, which can be attributed to the higher specific surface of the CA. Both the nucleation period and the reaction rate after the onset of the massive precipitation are higher at higher temperature.

Chemical shrinkage can be calculated using the stoichiometry of the individual hydration reactions, the density of hydration products and reactants and the degree of conversion for each reaction. Model predictions of chemical shrinkage based on the main reaction scheme of the CA hydration are in reasonable agreement with the experimental results. More data are needed to additionally validate the used model for predicting the chemical shrinkage evolution during continuous hydration, especially at higher temperatures when initially formed metastable hydration products transform to stable ones. The presented modeling methodology can be extended to develop more complex models to describe all reactions simultaneously, and even to include other hydraulically active minerals (e.g. $C_{12}A_7$, C_4AF and

C_2S). For such models more quantitative data on hydration of each mineral are needed.

Acknowledgement

The authors acknowledge support from the Croatian Ministry of Science, Education and Sports under project's no. 125-1252970-2983 "Development of hydration process model" and thank Calucem, Croatia for providing CAC samples.

References

- Bensted J. Calcium Aluminate Cements, Chapter 4 in Structure and Performance of Cements. 2nd edn, Bensted J, Barnes P, editors. London. 2002; 114-138.
- Fentiman C, Mangabhai RJ. *Proc. Int. Conf. on CAC*, Chapman and Hall, London. 2014.
- Mangabhai RJ, Glasser FP. *Proc. Int. Conf. on CAC*. Edinburgh, UK. 2001.
- Scrivener KL, Cabiron JL, Letourneux R. High-performance concretes from calcium aluminate cements. *Cement and Concrete Research*. 1999; 29: 1215-1223.
- Scrivener KL, Capmas A. Calcium Aluminate Cements, Chapter 13 in Lea's Chemistry of Cement and Concrete, 4th edn. PC Hewlett, John Wiley & Sons, NY, 1998.
- George CM. Industrial aluminous cements in Structure and Performance of Cements. Barnes P, editor. Applied Science, London. 1983. 415-470.
- Ukrainczyk N, Rogina A. Styrene-Butadiene Latex Modified Calcium Aluminate Cement Mortar. *Cement and Concrete Composites*. 2013; 41: 16-23.
- Ukrainczyk, N. Effect of Polycarboxylate superplasticizer on properties of Calcium aluminate cement mortar. to be published in *Advances in Cement Research*. 2014; 26: 1-10.
- Ukrainczyk N, Matusinović T. Thermal Properties of Hydrating Calcium Aluminate Cement Pastes. *Cement and Concrete Research*. 2010; 40: 128-136.
- Ukrainczyk N, Matusinović T, Kurajica S, Zimmermann B, Šipušić J. Dehydration of a Layered Double Hydroxide- C_2AH_8 . *Thermochimica Acta*. 2007; 464: 7-15.
- Sant G, Lura P, Weiss WJ. Measurement of volume change in cementitious materials at early ages: review of testing protocols and interpretation of results. *Trans. Res. Board Rec*. 2006; 1979: 21-29.
- Ideker JH, Folliard KJ, Thomas MDA. Early-age properties of calcium aluminate cement concrete with rigid cracking and free shrinkage frames: isothermal testing, *Calcium Aluminate Cements: Proceedings of the Centenary Conference*. Fentiman CH, Mangabhai RJ, Scrivener KL, editors. HIS BRE Press. 2008.
- Ideker JH. Early-age behavior of calcium aluminate cement systems [Dissertation]. The University of Texas at Austin. 2008.
- Mounanga P, Khelidj A, Loukili A, Baroghel-Bouny V. Predicting $Ca(OH)_2$ content and chemical shrinkage of hydrating cement pastes using analytical approach. *Cement and Concrete Research*. 2004; 34: 255-265.
- Ukrainczyk, N. Kinetic Modeling of Calcium Aluminate Cement Hydration. *Chemical Engineering Science*. 2010; 65: 5605-5614.
- George CM. Manufacture and Performance of Aluminous Cement: a New Perspective. Mangabhai RJ, editors. *Proc. Int. Conf. on CAC*, Chapman and Hall, London, 1990; 181-207.
- Ukrainczyk N, Vrbos N, Šipušić J. Influence of Metal Chloride Salts on Calcium Aluminate Cement Hydration. *Advances in cement research* 2012; 24: 249-262.
- Sipusic J, Ukrainczyk N, Vrbos N. Compressive Strength of Calcium Aluminate Mortar Determined by Ultrasonic Non-destructive Test Method. *Advances in Cement Research* 2013; 25: 143-154.

19. Matusinovic T, Sipusic J, Vrbos N. Porosity–strength relation in calcium aluminate cement pastes. *Cement and Concrete Research* 2003; 33: 1801–1806.
20. Ukrainczyk N, Matusinović, T. Modeling of Solid Fraction Evolution During Calcium Aluminate Cement Hydration. *International Conference On Material Science and 64th RILEM Annual Week In Aachen – Matsci, Aachen, Germany*. 2010. 189-198.
21. Geiker M, Knudsen T. Chemical shrinkage of Portland cement pastes. *Cement and Concrete Research*. 1982; 12: 603–610.
22. Knudsen T, Geiker M. Obtaining hydration data by measurement of chemical shrinkage with an archimeter. *Cement and Concrete Research*. 1985; 15: 381–382.
23. Geiker M. Studies of Portland Cement Hydration: Measurements of Chemical Shrinkage and a Systematic Evaluation of Hydration Curves by Means of the Dispersion Model. Technical University of Denmark, Copenhagen, Denmark. [Dissertation]. 1983.
24. Chung FH. Quantitative interpretation of X-ray diffraction patterns of mixtures. I. Matrix-Flushing Method for Quantitative Multicomponent analysis. *Journal of Applied Crystallography*. 1974; 7: 519-525.
25. Midgley HG. Quantitative Determination of Phases in High Alumina Cement Clinkers by X-ray Diffraction. *Cement Concrete Research*. 1976; 6: 217-224.
26. Lea FM. *The Chemistry of Cement and Concrete*, 3rd ed. Edward Arnold, London, 1976.
27. Bentz DP. Cellular automaton simulations of cement hydration and microstructure development. *Modelling Simul Mater. Sci. Eng.* 1994; 2: 783-808.